Current Biology, Volume *24*

Supplemental Information

Specialized Myrmecophily at the Ecological Dawn of Modern Ants

Joseph Parker and David A. Grimaldi

Systematic Palaeontology

Family Staphylinidae Latreille, 1802

Subfamily Pselaphinae Latreille, 1802

Supertribe Clavigeritae Leach, 1815

Revised diagnosis (modified from Chandler [S1]). Head with 3-8 antennomeres, terminal antennomere with setose cavity in truncate apex (cavity absent in *Colilodion*, *Articerodes*, *Kurbatoviella*, *Disarthricerus* and possibly others); lacking ocular mandibular carinae; mouthparts small, barely visible; maxillary palpi small, often with only one segment. Pronotum lacking paranotal carinae. Abdomen with visible tergites IV–VI fused into a tergal plate (tergites unfused in *Protoclaviger*). Paratergites IV (paratergites IV–VI in *Protoclaviger*) bearing tufts of specialized setae (trichomes). Legs with trochanters of middle and hind legs elongate, dorsal junction of mesofemur and mesotrochanter distant from mesocoxa; third tarsomeres longer than length of basal two tarsomeres combined, first and second tarsomeres subequal in length (second tarsomeres elongate in *Colilodion*), with single tarsal claws.

Comments. Creation of the new tribe Protoclavigerini brings the number of Clavigeritae tribes to four and necessitates a revised supertribal diagnosis. Morphological characters of the basal abdomen (the basal sulcus and basal fovea) [S1] are omitted since their form varies substantially across extant Clavigeritae, and these characters are not visible in *Protoclaviger*. Symmetric male genitalia [S1] is removed from the supertribal diagnosis because *Pseudacerus* [S2] and some undescribed New Caledonian species (P. Hlavac, personal communication) have since been discovered to possess asymmetric median lobes.

Tribe Protoclavigerini trib. nov.

Type genus: *Protoclaviger* Parker & Grimaldi here designated.

Diagnosis. Clavigerite pselaphines distinguished from all other Clavigeritae by possession of distinct, unfused tergites IV–VI; further distinguished by possession of 8 antennomeres, maxillary palpi emerging well outside buccal cavity, presence of paired hook-like trichomes on paratergites IV and V with smaller trichome on VI, and partially overlapping sternites indicating abdominal flexibility.

***Protoclaviger* gen. nov.**

Type species: *Protoclaviger trichodens* sp. nov., here designated.

Diagnosis. *Protoclaviger*, with its single species *P. trichodens*, is presently the only known genus of Protoclavigerini. At this time, diagnoses of the new genus and species thus match the tribal diagnosis above.

Description. Body length ~1.6 mm (Fig 1A, B), body form somewhat flattened dorsoventrally.

Head: Length: ~0.3 mm. Width across eyes: ~0.2 mm. Form triangular in lateral view, expanding apically to flat, steep frontal margin (Fig 1C). Vertex convex, raised and narrowed from eyes to clypeus to form short, prominent frontal rostrum. Vertexal fovea absent or not apparent (possibly obscured by trapped film of air). Lateral margins of head in dorsal view tapering weakly behind eyes to occipital constriction. Occipital carina absent. Neck largely hidden dorsally by pronotum. Gular area relatively flat, gular sulcus or fovea absent or not apparent. Neck ventrally exposed and broadening from occipital constriction to apical margin of prosternum. Eyes prominent (Fig 1C), positioned along lateral margins of head, crescent-shaped with ocular canthi formed from genal projection; ventral half of eye crescent extending into gular area. Region anterior to eyes excavate to form frontal rostrum. Antenna received under roof of frontal rostrum (Fig 1D, 3A). Antenna 8-segmented, antennomere 1 relatively large and exposed, easily visible (Fig 1D, 3A), antennal club formed by

enlarged antennomere 8 (Fig 1D, 3A). Apex of antennomere 8 abruptly truncate (Fig 1D) with apical face forming a recessed cavity (Fig 1E). Mandibular apex relatively blunt and weakly directed adorally, protruding slightly outside of buccal cavity (Fig 3A). Maxillary palpus projecting from side of buccal cavity; palpus evident as a single small, curved spatulate segment with truncate apex (Fig 3A). Setiferous brushes of maxillary galea/lacinia protruding from buccal cavity (Fig 1C).

Thorax: Pronotum length ~0.3 mm, width ~0.3 mm at widest point. 1.3x wider than head. Lateral margins smoothly rounded, broadening to just over half pronotum length before narrowing slightly to base (Fig 1B). Basal margin of pronotum angled convexly in outline, received between sloping elytral bases. Depressions at base evident, perhaps corresponding to median antebasal fovea and lateral antebasal foveae. Mesoventral-metaventral area strongly convex, with metaventrite sloping to apical margin in lateral view (Fig 1A). Metaventral apex produced between metacoxae into broad shelf that covers base of sternite III (visible ventrite 1). Ventral thoracic foveae unobservable.

Abdomen: Abdomen length ~0.6 mm, width at base ~0.6 mm slightly narrower than elytra and with dorsal surface strongly flattened. Three tergites (IV–VI) clearly evident, with distinct boundaries between them (Fig 1G). Broad paratergites present on all three segments. Thick, hook-shaped trichomes emerging from paratergites IV and V (Fig 1F, G), with smaller cluster of shorter setae present on paratergite VI (Fig 1F). Tergites IV and V subequal in length, VI 1.4x longer. Apical edges of tergites IV and V approximately straight to shallowly concave in outline; edge of VII broadly and convexly rounded (Fig 1G). Tergite VII barely visible in dorsal view, covered by apical margin of VI. Abdomen ventrally with six visible sternites (III–VIII). Sternites seemingly articulating (Fig 1A), with extensive intersegmental membrane indicated by apical edge of each sternite overlapping the base of the proceeding sternite. Sternite III short, 0.4x length of IV but extending well past metacoxae and spanning entire width of abdomen. Sternite IV longest, 1.2x V; V and VI subequal in length. Sternite VII shorter, 0.6x V; VIII smallest, 0.5x VII.

Legs: Procoxae contiguous, mesocoxae moderately separated, metacoxae separated by one-third metaventral width. Trochanters of all legs elongate ("macrosceline-type"), with femur distant from coxa. Femora and tibiae flattened, and broadened apically. Femora with apical excavation for retracted tibiae. Tarsi with tarsomeres 1 and 2 very short (I difficult to see within surrounding tibia apex); tarsomere 3 much longer (Fig 1H). Single tarsal claws.

Elytra: Elytral length ~0.5 mm; width at widest point ~0.3 mm, strongly convex in lateral view. Elytral bases sloping shallowly from humeri to midline. Lateral margins smooth and rounded, broadening from base to three-quarters elytral length before narrowing slightly to apex; apical elytral margins sinuate (Fig 1G). Elytra without evidence of any fovea or striae.

Protoclaviger trichodens sp. nov.

Holotype Material. Sex unknown (putative male). Data label: INDIA: Gujarat Tadkeshwar lignite mine. Cambay Form. (Paleo-Eocene) 21°21.400'N, 73°4.532'E Jan 11-16, 2012 Grimaldi/Nascimbene/Singh/Barden/Tribull/ Luzzi/Rana No. Tad-490. Specimen in AMNH.

Description. Body length 1.56 mm (Fig 1A, B, S1B). Colour uniform blackish brown, most dorsal surfaces coated with short, sparse, moderately aciculate pubescence.

Head: Length: 0.28 mm, width across eyes: 0.2 mm. Vertex with rugose sculpture (Fig 1C), covered with moderately dense, short erect setae orientated posteriorly. Median gular region with several short erect setae orientated slightly anteriorly. Eye (Fig 1C) with approximately 23 facets, ommatidia large, with golden sheen. Antenna (Fig 1D) 0.52 mm

long. Antennomere 1 subquadrate; 2 cylindrical, narrower than 1, 1.5x wider than long; 3–7 conical with ventral edges straight and dorsal edges curved (Fig 1D), 3–6 subequal in length and width, 7 larger. Dorsal faces of antennomeres 3–6 each with one or two prominent bristles pointing apically (Fig 1D). Dorsal and ventral regions of antennomere 7 apex each with cluster of 3–4 thick, blunt setae; antennomere 8 largest, equal in length to 6+7 combined; concave apex of antennomere 8 densely covered in short, thick setae and several longer setae (Fig 1D, E).

***Thorax*:** Pronotum length 0.26 mm, width 0.28 mm at widest point. Venter of thoracic segments lacking pubescence.

***Abdomen*:** Abdomen length 0.57 mm, width at base 0.56 mm. Trichomes on paratergites IV and V and trichome-like cluster on VI, all formed from shining, golden brown hair-like setae (Fig 1F). Medial tergite regions with short, sparse setae, some appearing large and flattened, possibly squamous-type. Sternites IV–VI with short setation on basolateral regions; IV and V also with medial regions sparsely setiferous.

Elytra: Elytron length 0.51 mm; width at widest point 0.3 mm, Uniformly covered with sparse, short setae.

Legs: Setae on tibiae and femora short, sparse and aciculate; longer, thicker setae around apex and on dorsal face of metatibia. Middle of ventral face of metafemora bearing distinct bract of 2–3 short, very thick bristles, possibly indicating the specimen is male.

Horizon and locality. The amber in which *Protoclaviger* is preserved was collected from outcrops exposed within large lignite mines in Gujarat state, western India, Tadkeshwar (N 21° 21.400', E 073° 4.532'), which cuts through extensive sequences of the Cambay Shale Formation, a 75-1500 m-thick layer of dense, glauconitic clay with seams of lignite, which was deposited in an intracratonic graben that trends NNW-SSE, called the Cambay Basin. The lowermost basin fill units are the Paleocene-Lower Eocene-aged Vagadkhol Formation (and its equivalent, the Olpad Formation), which directly overlies the Deccan Traps. These are overlain by the Late Paleocene-Middle Eocene-aged Cambay Formation, which can be subdivided into the Older Cambay Shale and the Younger Cambay Shale. In the Vastan mine is a 20-145 m thick unit of interbedded lignite beds, shales, carbonates, and clay-marls, which is lithologically equivalent to the Older Cambay Shale. A mid- to early-Ypresian age (ca. 50-52 Ma) of the Older Cambay is indicated by fossil shark teeth and by the index foraminiferan *Nummulites b. burdigalensis*, found between the upper and lower lignite seams at Vastan. In the Cambay Shale system, sediment input was probably seasonal with an equatorial climate, and the bulk of the sediment derived from chemical weathering of the thick Deccan Traps. Nature of the sediments suggests deposition in a low-energy, nearshore/coastal setting similar to extensive 1600-km long chenier systems along the coast of northeastern South America. Dense mangrove forests fringed the coast of the Eocene muddy shelf that formed the Cambay shale, with large dipterocarp forests further inland where the amber was formed.

Supplementary Discussion

Systematic and functional morphology of *Protoclaviger*

It is evident on first sight that *Protoclaviger* represents a transitional form between the morphologically derived myrmecophilous Clavigeritae and largely free-living ancestral Pselaphinae. In addition to possessing the same overall habitus as most Clavigeritae, *Protoclaviger* exhibits key synapomorphies that support its phylogenetic affinity to this supertribe. Several such characters serve adaptive functions inside ant colonies, and thus testify to *Protoclaviger*'s likely myrmecophilous biology. Importantly however, certain autapomorphies of Recent Clavigeritae are missing in *Protoclaviger*, while others are present at an intermediate state of evolutionary development. In what follows, important functional and diagnostic characters of Recent Clavigeritae are compared to the states found in *Protoclaviger*. Reference is made to Figures S1 that shows confocal reconstructions of a typical clavigerite, *Diartiger fossulatus*, from Japan.

1. Abdominal trichomes. Recent Clavigeritae possess trichomes—dense, elaborately sculpted brushes of yellow hair-like setae—at the base of the abdomen. Trichomes typically emerge from paratergites IV (flanking the first visible tergite) (Fig S1D, E). In some genera, additional trichomes also emerge from within tergite IV itself, or from the posterior margin of the elytron. Trichomes act as wicks, conducting substances from large "Wasmann glands" embedded at the base of the abdomen [SS3-5]. The substances themselves are unidentified, but host ants find them attractive and are commonly observed licking the trichomes (Supplemental Video S3). Trichome exudate is thought to appease the ant, and induce it to feed the beetle via stomodeal trophallaxis [S6]. Trichomes are also positioned at a part of the beetle's body that is fashioned into a "grasping notch" [S7], used by worker ants to pick the beetles up and carry them around inside the nest (Fig 2B; Supplemental Video S2). Analogous trichome structures have arisen in some other obligately myrmecophilous beetle taxa, including chlamydopsine histerids, paussine carabids, cremastocheiline scarabaeids, lomechusine staphylinids, as well as in scattered other Pselaphinae genera (e.g. *Attapsenius*, *Epicaris*, *Desimia*, *Janusculus*, *Baceysus*, *Batrisiotes*, *Dendrolasiophilus*, *Gadgarra*, *Songius*, *Millaa*). When the biology is unknown, trichomes are a reliable indicator that a given species is myrmecophilous. They are the "badges" of the socially integrated myrmecophile [S8].

Protoclaviger bears dense bundles of yellow setae forming hooked-shaped trichomes in exactly the same position as Recent Clavigeritae—on paratergites IV (Fig 1F). Additionally, *Protoclaviger* has trichomes on paratergites V, and smaller trichome-like tufts on paratergites VI (Fig 1F). We propose that trichomes may have initially developed as serially homologous structures on abdominal segments IV-VI, before the derived modification of the abdomen in crown-group Clavigeritae restricted trichome development to paratergites IV alone. Trichomes on the elytral margins and within tergite IV, seen in some genera of Recent Clavigeritae, would then represent derived additions to the symplesiomorphic trichomes emerging from the paratergites.

2. Abdominal "tergal plate". The first three visible tergites (IV–VI) of all Recent Clavigeritae are fused into a composite tergal plate (Fig S1D). Fusion of the tergites may strengthen the abdomen when the beetle is being carried or licked by host ants, and may also facilitate the spreading of exudates from the Wasmann glands and other glandular units that decorate the abdomen [S5]. Remarkably, in *Protoclaviger*, the tergites are distinct, with true segment boundaries plainly evident (Fig 1G). A further difference lies in the relative lengths of the dorsal abdominal segments. Unlike the tergites, the paratergites in Recent Clavigeritae are still demarcated by

boundaries, and thus betray the relative lengths of the segments to which they belong (Fig S1D). The paratergites reveal that tergite IV typically exceeds the length of V, which is subequal in length to or longer than VI. In contrast, *Protoclaviger* has tergite IV and V subequal in length, while tergite VI is the longest (Fig 1G). Hence, the overt restructuring of the abdomen of Recent Clavigeritae is not seen in *Protoclaviger* with its largely primitive tergite morphology. However, *Protoclaviger*'s broad, relatively flat tergites may anticipate the very wide and often flattened form of the tergal plate of Recent Clavigeritae. Whether *Protoclaviger* possesses the deep basal excavation of tergite IV seen in Recent Clavigeritae [S1] cannot be ascertained at this time, due to the elytra covering the abdomen base, as well as damage to the right hand side of the abdomen (Fig 1G).

3. Abdominal intersegmental membranes. Although the abdominal segments of Recent Clavigeritae are still distinct ventrally, their intersegmental membranes are extremely short [S9]. Neighbouring sternites appear to be fully contiguous with each other (Fig S1F), and in lateral view, the abdomen has a smooth, continuous ventral profile, uninterrupted by obvious segment boundaries. Reduction of membrane creates a ventrally rigid abdomen, matching the absolute immobility of the fused, dorsal tergites IV–VI. *Protoclaviger*, like non-clavigerite Pselaphinae, has extensive intersegmental membranes, so the sternites appear to be partially articulating (Fig 1A). This flexibility of the ventral abdomen matches *Protoclaviger*'s still-distinct and possibly articulating tergites IV–VI (Fig 1G).

4. Antennomere consolidation. Most pselaphines possess 11 antennomeres, whereas Clavigeritae have between three and six through loss of a varying subset of antennomere pedicels and seamless fusion of the segments (Fig S1A, C; note that *Diartiger fossulatus* has four antennomeres but the minute scape is not visible in these images). Like trichomes, consolidation or compaction of antennomeres is common among myrmecophilous beetles [S10-12], and presumably strengthens the antenna, protecting against damage or loss of segments when the beetle is gripped by ant mandibles. Evolutionary loss of the pedicels also increases the surface area for the development of exocrine glands [S6], and may facilitate the spreading of exocrine secretions across an uninterrupted integument. *Protoclaviger* possesses 8 antennomeres—a degree of antennomere consolidation intermediate between other Pselaphinae and Recent Clavigeritae.

5. Reduced antennomere pedicels. An additional means of antennomere consolidation is achieved by reducing/concealing the thin antennomere pedicels that form the junctions between any remaining, still-distinct antennomeres (Fig S1A, C). This gives the antenna the distinctive appearance of a stacked set of inverted cones. As in Recent Clavigeritae, the antennomere pedicels are indistinct in *Protoclaviger*, and the conical form of the antennomeres is identical (Fig 1D).

7. Truncate antennal apex with setose cavity. The tip of the antenna of Clavigeritae is characteristically truncate and excavate, with the apical cavity filled with short, thick setae (Fig S1C and inset). The apex is covered with glandular units that ants lick and may encourage trophallaxis from ant to beetle [S6]. In Clavigeritae, the setose cavity is known to be absent in a few genera, but these still have the apex relatively truncate and covered with short, thick setae. *Protoclaviger* possesses the stereotypical apically truncate, setae-filled excavation of the vast majority of Recent Clavigeritae (Fig 1D, E). We regard the absence of the cavity in some Recent genera as a derived loss.

8. Antennal scape. Recent Clavigeritae typically have the derived condition of very short scapes (antennomeres 1), which are hidden when the head is viewed from above

or below, and do not extend past the shelf-like overhangs of the frontal rostrum (Fig S1A, B; note that the basal-most segment visible in these images is antennomere 2). In contrast, *Protoclaviger* has enlarged scapes, protruding out from under the frontal rostrum, akin to outgroup Pselaphinae (Fig 1D, Fig 3A).

9. Reduced mouthparts. Pselaphinae possess 4-segmented maxillary palpi with a 5th apical "pseudosegment"—an autapomorphy of the subfamily [S9]. The palpi are often large and elaborate, and in at least some species are used to trap moving prey items [S13]. Clavigeritae have miniscule maxillary palpi, reduced to a single main palpomere [S14] which does not extend outside of the confines of the buccal cavity (Fig S1B). Diminution of the palpi occurs in some other myrmecophilous or presumed myrmecophilous Pselaphinae (e.g. *Attapsenius* [S8] and some genera of Arhytodini) and may facilitate novel modes of feeding associated with this lifestyle. However, it could also be due to evolutionary degeneration, as enlarged palpi are no longer required for dealing with large, moving prey objects as the mode of feeding has shifted to trophallaxis and consuming immobile ant eggs and larvae. The maxillary palpi of *Protoclaviger* are comprised of a single main segment (Fig 3A), which is bent midway, in similar fashion to genera of Recent Clavigeritae (Fig 3B, S1B). The palpi are very small, but nonetheless still larger than those of Recent Clavigeritae, and they extend some way outside of the buccal cavity (Fig 3A). We interpret *Protoclaviger*'s maxillary palpi as transitional between those of ancestral Pselaphinae and Recent Clavigeritae. Similarly vestigial maxillary palpi—reduced to a single, bent segment that extends outside of the buccal cavity—occur in some genera of Arhytodini (the form seen in *Protoclaviger* is most closely approximated in *Sabarhytus* [S15]). This tribe, together with Pselaphini, are closely allied to Clavigeritae (Fig 3A, 4A). However, many other genera of and Arhytodini (and all genera of Pselaphini) possess plesiomorphic 4-segmented maxillary palpi, implying that palpomere reduction in some arhytodines may have arisen convergently, possibly in response to similar myrmecophilous lifestyles.

The mandibles of Recent Clavigeritae are only weakly toothed compared to other Pselaphinae [S14], consistent with their derived use in novel feeding modes such as piercing ant eggs and larval cuticles, scraping larval exudates, and feeding via trophallaxis [S8, 16]. The mandibles are also largely recessed inside the buccal cavity, with only their tips protruding outside. *Protoclaviger* also appears to have somewhat weakly toothed mandibles (Fig 3A), and the mandibles do not strongly protrude outside the buccal cavity, approaching the state seen in Recent Clavigeritae.

11. Tarsal morphology. Pselaphinae have 3-segmented tarsi, and in most groups, tarsomere 2 exceeds the length of tarsomere 1, which is usually extremely short. In Clavigeritae, tarsomeres 1 and 2 are both very short, and tarsomere 3 comprises most of the length of the tarsus (Fig S1I). A single tarsal claw is present. *Protoclaviger* has tarsi identical to those of Recent Clavigeritae (Fig 1H)—a clear synapomorphy. One genus of Clavigeritae, *Colilodion*, has tarsomere 2 elongate, like most other Pselaphinae, and this has led to the notion that *Colilodion* represents an evolutionary intermediate between Clavigeritae and outgroup Pselaphinae [S17-19]. Such a view is difficult to reconcile with *Protoclaviger*, which possesses a larger number of primitive character states than does *Colilodion*, and in our cladistic analysis forms the basal-most lineage within Clavigeritae (Fig 3C). If *Colilodion* is indeed a true member of Clavigeritae (a placement which has been questioned [S18]), its tarsal morphology is a derived character, and the product of a reversal to the ancestral condition seen elsewhere in Pselaphinae. Evaluation of *Colilodion*'s phylogenetic position within Pselaphinae awaits collection of DNA-grade

specimens of this extremely scarce South East Asian genus.

12. Additional characters for systematic placement of **Protoclaviger.** Like Recent Clavigeritae, *Protoclaviger* possesses elongate "macrosceline"-type trochanters on all legs, where the coxa and femur are distant from each other, and the joint between trochanter and femur is almost perpendicular to their longitudinal axes (Fig S1G, H) [S1]. Elongate trochanters also occur in Pselaphitae, so this character is not a synapomorphy linking *Protoclaviger* to Clavigeritae. However, their presence in *Protoclaviger* is nonetheless consistent with our phylogenetic placement of the new genus. The convex, ventrally protruding meso-metaventrite of *Protoclaviger* (Fig 1A) is also characteristic of the form seen in many Clavigeritae. It should also be noted that *Protoclaviger* has few foveae—internally striated pits that decorate the body of Pselaphinae in a stereotypical pattern, and which have important systematic value [S1]. Foveae may serve a structural purpose [S1], and the trend is for them to become evolutionarily lost in myrmecophilous taxa (e.g. [S1, 20-22]). Clavigeritae have a highly reduced number of foveae. Preservation precludes detailed examination of *Protoclaviger*'s foveation pattern, but there is little evidence of foveae in exposed positions: vertexal foveae (the dorsal tentorial pits), elytral foveae, and ventral thoracic foveae such as the lateral mesocoxal and lateral metaventral foveae, are not apparent. Lateral and medial antebasal foveae or depressions on the pronotum—which some Recent Clavigeritae possess—may be present, but these inferred structures could be artefacts caused by fossilization. Interestingly, the medial regions of the abdominal tergites appear to have blunt, flattened rectangular-shaped pubescence (Fig 1G). This kind of pubescence is wholly absent among genera of Recent Clavigeritae. It is very similar—perhaps homologous—to the squamous pubescence seen in Arhytodini and Pselaphini, the putative sister tribes of Clavigeritae

13. Autapomorphies of **Protoclaviger.** *Protoclaviger* presents a mostly transitional morphology with few evident autapomorphies. However, several structures may represent unique, derived characters. The thick bristles on the dorsal apex of antennomeres III–VI are distinctive (Fig 1D), although possibly only in their configuration rather than type, since thick bristles adorn the antennae of most Clavigeritae. The crescent-shaped eyes, bisected by deep ocular canthi (Fig 1C) are also notable but not unique in Clavigeritae (even more exaggerated "split" eyes are seen in *Colilodion* [S19]). The bract of thick, short setae on the metafemur— potentially a sex-linked character—is unusual, and perhaps autapomorphic. In Clavigeritae, it is typically the male mesoleg that bears similar structures, usually in the form of tubercles or spines on the tibia, femur or trochanter. Additionally, the dorsally convex ("hollowed out") form of the apex of the spatulate maxillary palpi (Fig 3A) is, to our knowledge, highly atypical, and a further possible autapomorphy. Finally, the apparent lack of vertexal foveae—a character present in some Recent Clavigeritae—may also represent a derived loss in *Protoclaviger*.

Given these unique traits, *Protoclaviger* may not be directly ancestral to Recent Clavigeritae, but rather a highly plesiomorphic member of the stem-group that diverged early, inheriting a body plan midway during the major remodelling that produced the crown-group form. Such a notion fits with our molecular dating analysis, which indicates that crown-group Clavigeritae may predate *Protoclaviger* by some 10 Ma (Fig 4A; see following discussion).

Phylogenetics and diversification of Clavigeritae

The apparent rareness of the vast majority of Clavigeritae in nature has been a major barrier to conducting any kind of phylogenetic analysis of this beetle taxon. We accumulated sufficient freshly-collected and dried museum material to allow the assembly of a 5-gene data set for almost 25% of recognised genera, enabling us to perform the first-ever phylogenetic analysis of Clavigeritae (molecular or otherwise). Our analysis includes 2 of the 3 tribes (Clavigerini and Tiracerini; only the vanishingly rare SE Asian monobasic Colilodionini—6 described species known from fewer than 20 specimens—was unavailable, but we discuss the implications of this taxon's absence). Within Clavigerini, we obtained representatives of 8 of the 10 subtribes (only Lunillina and Disarthricerina, were unavailable, and the absence of these obscure and probably derived subtribes does not likely influence our conclusions). We thus achieved a broad and taxonomically unbiased sample from across the supertribe, of sufficient density to infer the group's approximate pattern of diversification. The variable and heavily modified morphology of Clavigeritae has hindered attempts to confidently resolve the supertribe's relationship to other Pselaphinae; furthermore, within Clavigeritae itself, extraordinary morphological variation has precluded creation of a stable system of internal relationships. Our analysis is the first to explicitly study the relationship between Clavigeritae and other Pselaphinae, as well as the first to shed light on some key internal relationships.

We find that Clavigeritae are monophyletic (Fig 4A, S2), and form a well-supported relationship with the tribes Pselaphini and Arhytodini of the supertribe Pselaphitae. This scenario which has been alluded to by previous authors [S9, 17]. All tribes of Pselaphitae share with Clavigeritae the elongate ("macrosceline") trochanters, most clearly seen in the mesolegs, but Pselaphini and Arhytodini are distinct among Pselaphitae in possessing single tarsal claws, like Clavigeritae. Notably, both Pselaphini and Arhytodini also exhibit flattened "squamous"-type pubescence on various body regions. This kind of pubescence is absent among genera of Recent Clavigeritae, but *Protoclaviger* appears to have patches of squamous pubescence on the medial regions of tergites IV–VI, as seen in some genera of Arhytodini. This relationship between Clavigeritae and Arhytodini is congruent with results from a taxonomically comprehensive phylogenetic analysis of the entire Pselaphinae (~240 ingroup taxa from all supertribes and 37 of 39 tribes), to be published elsewhere (J. Parker, in preparation).

Within Clavigeritae, three tribes are presently recognised [S17]: Tiracerini, Colilodionini and Clavigerini. Our analysis supports the reciprocal monophyly of Tiracerini and Clavigerini (Fig 4A, S2), but the systematic position of Colilodionini could not be resolved at this time. Our morphological analysis (Fig 3C) places Colilodionini basal to (Tiracerini, Clavigerini)—a relationship we hope to test molecularly when DNA-grade specimens of *Colilodion* become available. Clavigerini, the largest tribe, currently contains 10 subtribes of questionable validity [S17]. Some are monobasic, while others bring together genera based on characters that are likely homoplasious, such as antennomere number and trichome position [S23, 24]. In our analysis, basal relationships within Clavigerini are relatively weakly supported, consistent with the tribe radiating quickly. However, consistent with the inadequacy of the subtribal classification system, the 10 included genera of the largest subtribe, Clavigerodina, are distributed across the tree in a way that is irreconcilable with the monophyly of this subtribe. Similarly, Besuchet's expanded concept of the subtribe Clavigerina [S25], based on the form of the basal excavation of the tergal plate and incorporating several genera including

Claviger, *Adranes*, *Diartiger* and *Triartiger*, is only partially supported. Our results confirm a relationship among *Diartiger*, *Triartiger* and *Adranes*, but do not support this clade grouping with *Claviger*. This raises the possibility that eyelessness evolved independently in the Palearctic *Claviger* and Nearctic *Adranes*. Monophyly of other subtribes including Apoderigerina and Mastigerina is also in conflict with our analysis. A detailed study of morphology in Clavigerini, guided by molecular data, is badly needed to create a new higher-level classification for this tribe.

In contrast to the lack of support for subtribes, our analysis reveals some unexpected relationships within Clavigerini. Notably, the Madagascan genera we included form a well-supported monophyletic group. Madagascar is home to a remarkably rich clavigerite fauna: 30 described genera are known to occur there, 29 of which are endemic [S26]. However, estimating their relationships has historically been impeded by dramatic morphological variation, leading some authors to erect new subtribes and even new tribes to accommodate particularly enigmatic genera [S23, 24]. Our results are consistent with Clavigeritae having undergone an unprecedented radiation within the confines of the Madagascan landmass, but further taxon sampling from the Island's clavigerite fauna, as well from the continental Afrotropics, will be needed to fully test this hypothesis. Other relationships elsewhere in Clavigerini are also notable. The genus *Fustiger* is polymorphic and diagnosed by extremely weak criteria: a New World geographic occurrence, and possession of three antennomeres (many Old World genera of Clavigeritae have three antennomeres). Surprisingly, our five included representatives of *Fustiger* from the USA, Costa Rica, Peru and Brazil do form a clade, indicating that *Fustiger* may in fact be monophyletic. It is possible that *Fustiger* represents a largely Neotropical radiation of equivalent species richness to that of Madagascar, albeit morphologically more conservative.

Our dating analysis using BEAST illuminates the temporal sequence of clavigerite diversification. We infer a date for the clavigerite stem of 73 Ma, followed by a short, ~11 Ma period of stem evolution, and a crown-group age estimate for Clavigeritae of ~62 Ma. This crown-group age predates *Protoclaviger* (dated to 52 Ma), indicating that *Protoclaviger* may belong to a stem lineage that diverged between 73–62 Ma, persisting alongside crown-group Clavigeritae until at least the early Eocene. Since our analysis did not include *Colilodion*, a crown-group genus that may be sister to the (Tiracerini, Clavigerini) clade (Fig 3C), the actual period of stem-group evolution may be shorter still. Our topology places Indomalayan and Australasian genera basal within Clavigeritae, which together with *Protoclaviger* in Indian amber, indicates that this region may be the group's evolutionary center of origin. We infer that, from this region, Clavigeritae reached Madagascar and began radiating 43–37 Ma, and reached the New World on at least two independent occasions, once to form *Fustiger* (37–29 Ma), and slightly later to form *Adranes* (35–12 Ma). The exclusively Nearctic range of the latter genus, and its affinity to the East Asian *Diartiger* and *Triartiger*, suggest a possible Beringian route into North America. One future avenue of study will be to correlate the global spread of Clavigeritae with the historical dispersal of their host ants.

Our inferences about the temporal dynamics of diversification are based on a BEAST analysis with relatively non-stringent fossil calibrations (Analysis #1; see Materials and Methods). To explore the effects of our fossil constraints, we performed an otherwise identical BEAST run but with tighter priors (Analysis #2), which led to comparable results for the radiation of Clavigeritae (Fig S4A), with only slightly younger ages for stem- and crown-group Clavigeritae (Fig S4G). In contrast, testing whether our priors alone (Analysis #3; Fig S4B) or the molecular data

without fossil calibrations (Analysis #4; Fig S4C) were constraining the outcome of our analysis [S23, 24, 27, 28] led to vast differences in age estimates (Fig S4B, C, G). Hence, our inferences concerning the origin and diversification of Clavigeritae are not driven by either overly-strong priors or molecular data, but are instead the outcome of the priors and molecular data working synergistically. Notably, performing additional analyses depicted in Figure S4H, using an alternative placement of fossil A (Arhytodini), or without fossils A and E (*Protoclaviger*), yields age estimates for stem- and crown-group Clavigeritae that are slightly older than those obtained in our focal analysis (Fig S4D, E, G). Hence, we conclude with confidence that our inferred age for the origin of obligate myrmecophily in Clavigeritae is, if anything, conservative, and the lifestyle may be slightly older still. Finally, running the analysis without constraining the topology yielded a tree that differed only in several weakly-supported regions within the Clavigeritae clade, and produced a near-identical lineages through time plot (Fig S4F). Hence, our inferences concerning the diversification of Clavigeritae are not contingent on our constraint tree, and are robust to any weakly-supported internal relationships inside Clavigeritae.

Lastly, we do not think that increased taxon sampling will fundamentally alter our conclusions. Our taxon sampling is spread in an unbiased fashion across the higher classification of Clavigeritae, and not concentrated on one group in particular. More importantly, we see already from our analysis, using ~25% of genera from the supertribe, that Clavigeritae begin radiating soon after they first arise; hence, there is no long branch leading up to their radiation that addition of further taxa might "break up". It is possible that addition of further taxa might benignly alter their inferred rate of diversification, but this would not negate our hypothesis for when the group arose, and our finding that they experienced a radiation from approximately the Paleocene/early Eocene until approaching the present day (Fig 4A, B).

The myrmecophile fossil record

The general scarcity of myrmecophiles relative to other arthropods means they are mostly known from only the richest fossil deposits. Our survey of described and undescribed fossil myrmecophiles indicates that *Protoclaviger*, in Ypressian-age Cambay amber (~52 Ma) is demonstrably the oldest-known myrmecophile. The next oldest myrmecophiles occur in Lutetian Baltic amber, ~8–10 Ma younger than Cambay amber. Pselaphinae of the tribes Tmesiphorini, Ctenistini and Batrisini have been described [S29], all of which contain obligately myrmecophilous extant species, although none as highly socially-integrated as Clavigeritae. Paussine carabids of the tribe Paussini—another large, Recent group of obligate myrmecophiles—are also known from Baltic amber [S30] (also found as compression fossils in the contemporaneous Eckfelder Maar of Germany [S31]). The presence of these putative myrmecophiles is consistent with the high ant diversity of Baltic amber [S32] and increasing ecological presence of ants by the middle to late Eocene [S33, 34]. Although not socially-integrated myrmecophiles, Baltic amber also contains an adult wasp of the family Eucharitidae [S35], modern members of which have larvae that are endo- and ectoparasitoids of ants, and a putatively parasitic mesostigmatid mite [S66].

The late Eocene (Priabonian) Bembridge Marls fossils (Isle of Wight, UK) include a butterfly, *Lithopsyche antiqua* Butler, a questionable member of Lycaenidae [S36], many Recent members of which have socially parasitic caterpillars. The earliest definitive record of Lycaenidae is *Aquisextana irenaei* Théobald, from the late Oligocene/Early Miocene (Chattian–Aquitanian) of Aix-en-Provence (France) [S36]. This deposit also provides the first record of an adult *Microdon* [S37], a hover fly genus (Syrphidae) with

myrmecophilous larvae. Mexican amber of approximately the same age, as well as slightly younger Domincan amber from the early Miocene (Burdigalian; ~20 Ma), contain many putatively myrmecophilous groups, including Paussini [S38, 39] and haeteriine histerid beetles [S40], modern members of which include many guests of Neotropical army ants. Staphylinids of the subfamily Oxytelinae [S41], and Pselaphinae of the modern, putatively myrmecophilous genera *Rhytus*, *Caccoplectus* and *Pselaphomorphus* (specimens in the AMNH collection) have also been recovered from these ambers. The diversity of myrmecophiles in Dominican amber in particular, and their similarity to Recent forms, suggests a relatively complete collection of modern colony guests had arisen by at least ~20 Ma, consistent with the high percentage of ants in this tropical palaeoenvironment.

We reject the claim of Martins-Neto [S42] of Myrmecophilinae (Orthoptera) in the Cretaceous Crato formation of Brazil. Myrmecophilinae are a small group of specialised, myrmecophilous “ant crickets”. Like many Crato compressions, *Araripemyrmecophilops gracilis* Martins-Neto appears to be a cockroach. We mention also that a member of the pselaphine tribe Arhytodini has been recovered from Cambay amber (“Fossil A” in our dating analysis; Fig S3A). Some Arhytodini have small, recessed mouthparts suggesting a mode of trophallactic feeding similar to Clavigeritae [S43, 44]. Hence, these beetles are potentially myrmecophilous, although only a single report exists of their collection from ant colonies [S45]. Nevertheless, this arhytodine inclusion may thus represent the joint oldest-known myrmecophile, along with *Protoclaviger*. However, unlike *Protoclaviger*, the arhytodine fossil—which will be published elsewhere—has no unambiguous adaptive characters for myrmecophily, and unlike all Recent Arhytodini, has enlarged and morphologically elaborate mouthparts. Note that the recent placement of a mid-Cretaceous amber pselaphine in Arhytodini [S46] was erroneous, and a re-evaluation of its position will be published shortly.

Finally, we note that *Protoclaviger* represents the only definitive fossil of Clavigeritae thus far discovered. A specimen of *Articerus* Dalman has been documented in Copal, but is most probably a Recent species [S47].

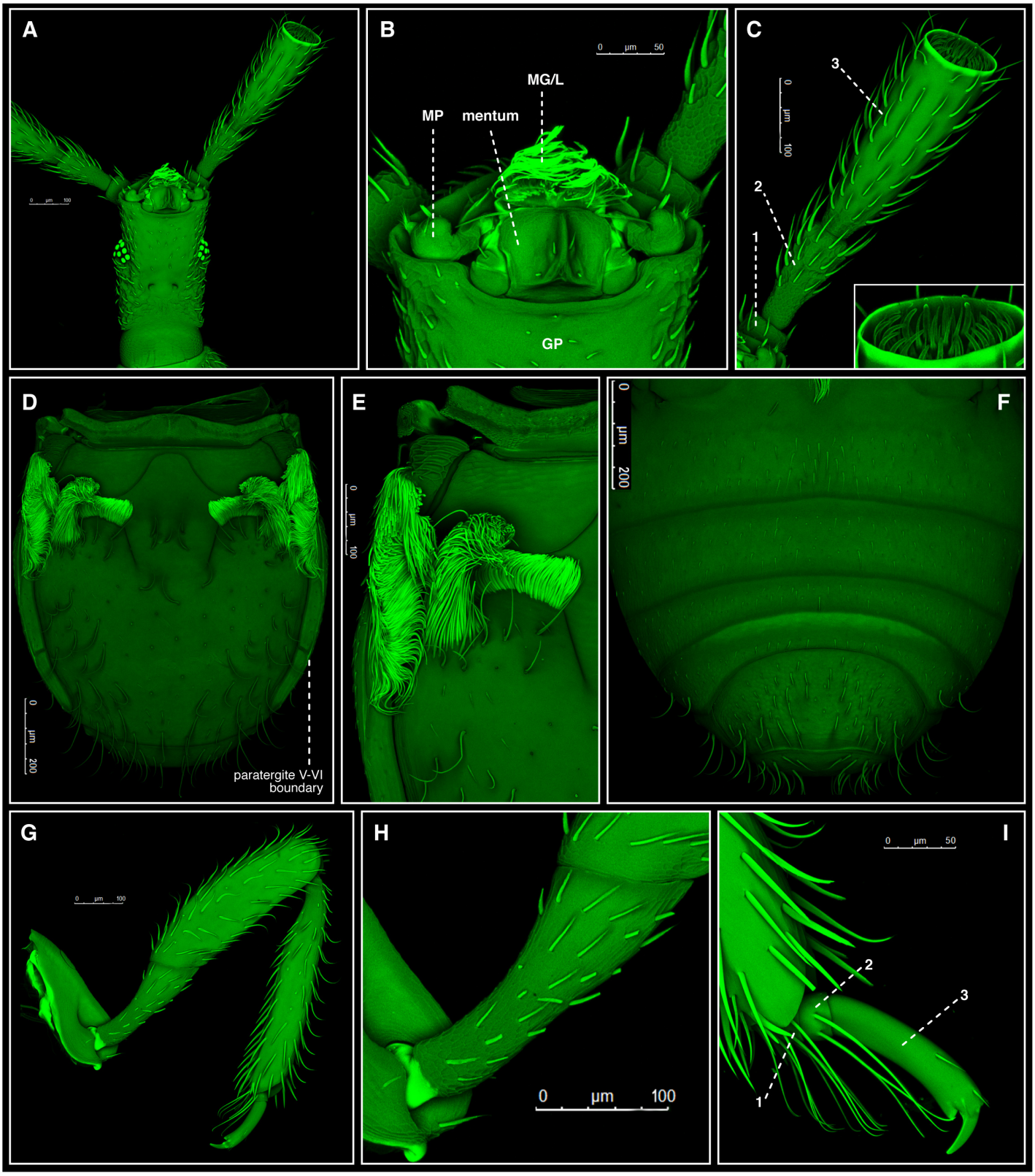

Figure S1. Morphology of Recent Clavigeritae (related to Figure 3). Confocal maximum projection images of *Diartiger fossulatus*. **A:** Head venter. **B:** Buccal cavity with maxillary galea/lacinia (MG/L), maxillary palp (MP) and gular plate (GP) indicated. **C:** Left antenna (ventral face) with antennomere number indicated. Inset shows close up of truncate, setose apical cavity. **D:** Dorsal abdomen showing tergal plate (fused tergites IV-VI), with boundary between paratergites V and VI indicated. **E:** Close up of left trichome. **F:** Ventral abdomen, showing apparent absence of intersegmental membranes. **G:** Left metaleg. **H:** Left metatrochanter. **I:** Left metatarsus, with tarsomeres indicated.

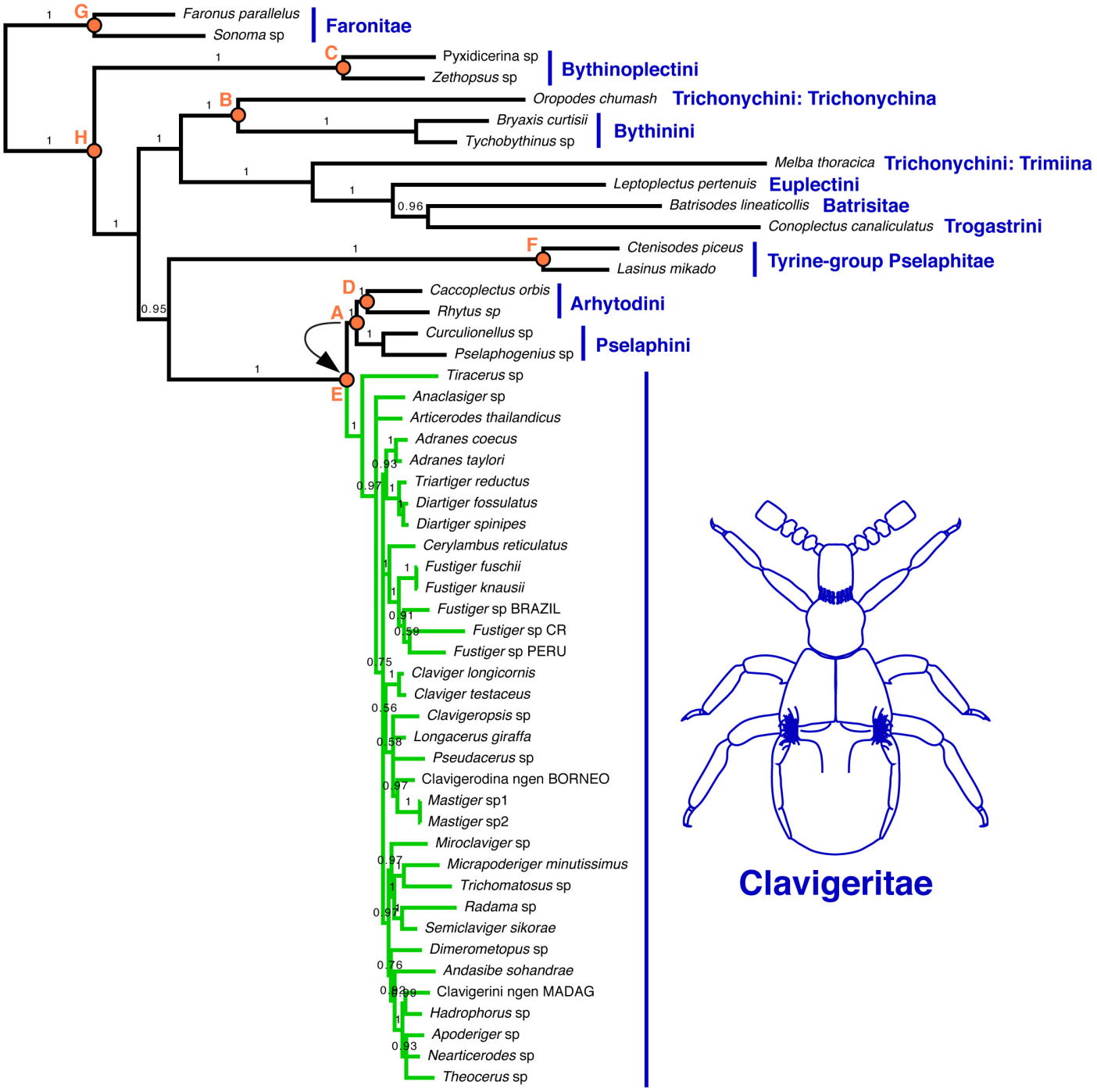

Figure S2. Bayesian phylogenetic tree of Clavigeritae and pselaphine outgroups (related to Figure 4). Consensus tree from the MrBayes analysis of the partitioned 5-locus data set. Numbers above branches are posterior probabilities. Fossil-calibrated nodes used in BEAST are indicated by orange circles, with letters denoting fossils listed in Materials and Methods. The arrow indicates the alternative placements of Fossil A used in BEAST analyses #1 and #5.

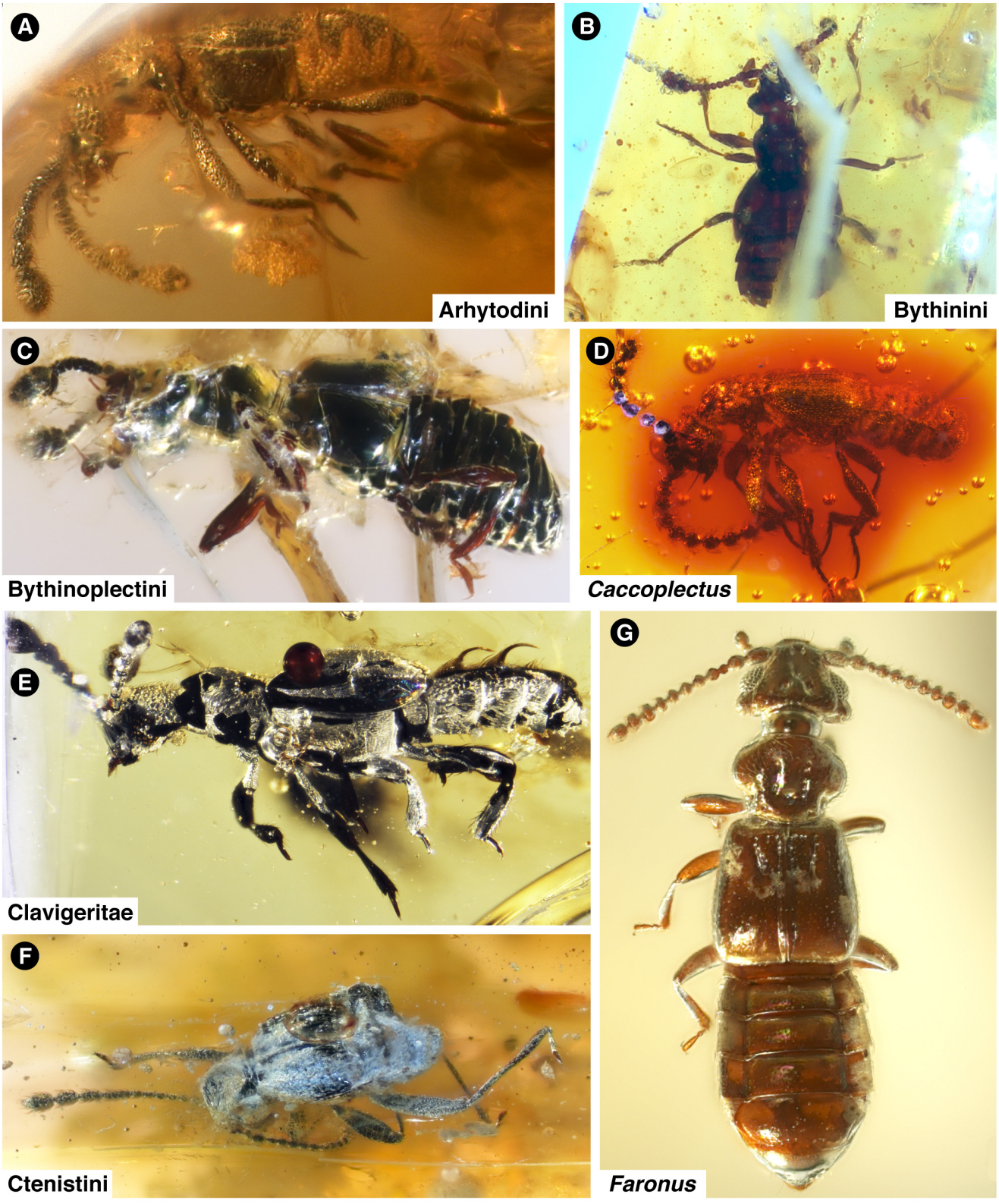

Figure S3. Amber Pselaphinae used for molecular dating (related to Figure 4). A: Fossil A (undescribed Arhytodini in Cambay amber; AMNH TAD-23). **B:** Fossil B (undescribed Bythinini in Burmese amber; AMNH B-023). **C:** Fossil C (undescribed Bythinoplectini: Bythinoplectina in Cambay amber; AMNH TAD-130). **D:** Fossil D (*Caccoplectus* in Dominican amber; AMNH DR8-429). **E:** Fossil E (*Protoclaviger* in Cambay amber; AMNH TAD 490). **F:** Fossil F (undescribed Ctenistini in Cambay amber; AMNH TAD-491). **G:** Fossil G (*Faronus* in Baltic amber AMNH Ba-JWJ 334).

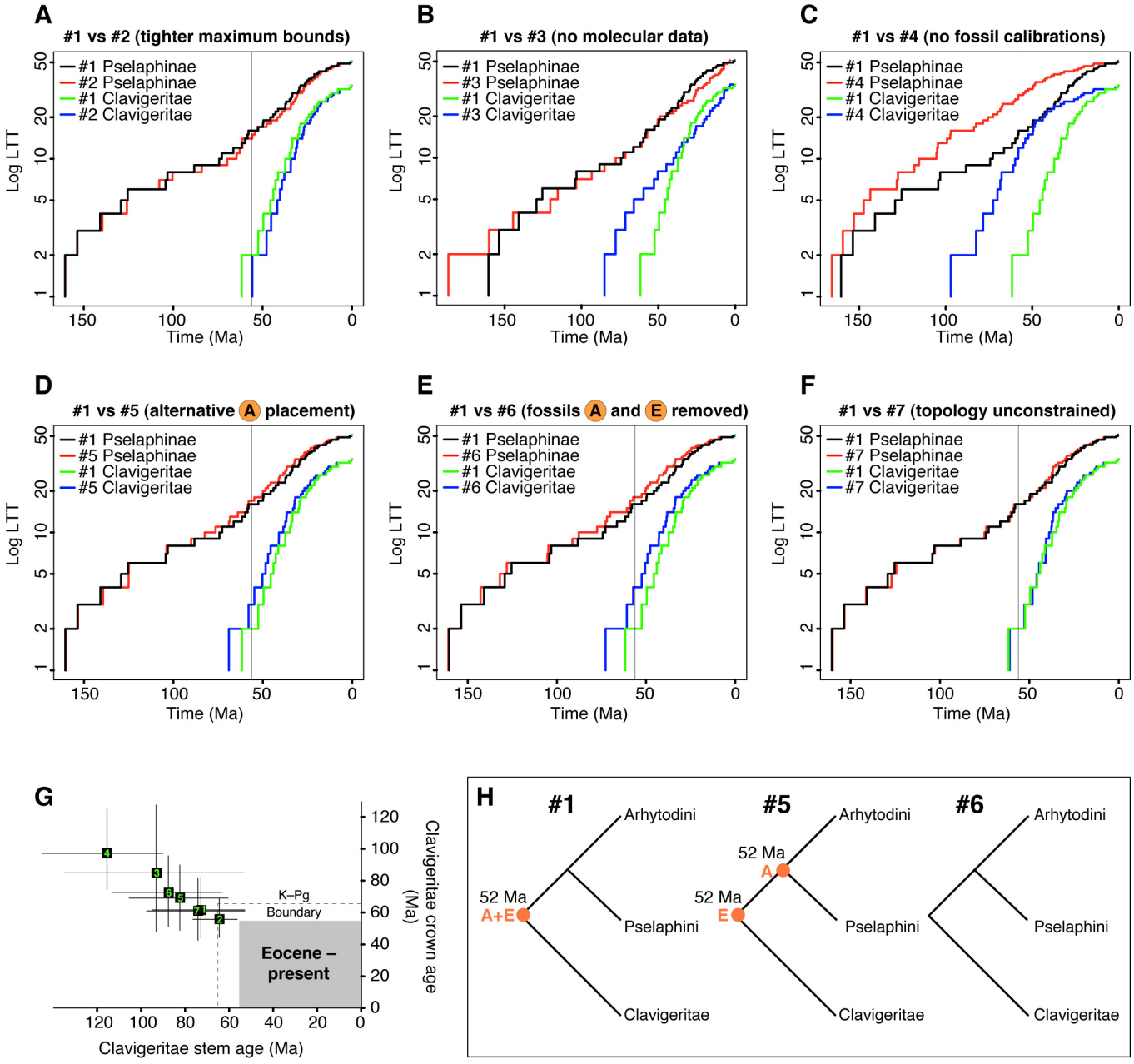

Figure S4. Effects of BEAST priors on date estimates (related to Figure 4). A-F: LTT plots from BEAST analysis #1 compared to analyses #2-7. Total Pselaphinae lineages are shown in addition to the crown-group Clavigeritae clade alone. The vertical line marks the Paleocene-Eocene boundary. **G:** Plot of Clavigeritae stem-group age vs crown-group age for analyses #1-7. Error bars are 95% HPD. **H:** Fossil placement schemes for Fossils A (Arhytodini) and E (*Protoclaviger*) in analyses #1, 5 and 6.

Experimental Procedures

Fossil collection and preparation

The holotype and unique specimen of *Protoclaviger* was discovered amidst approximately 20 kgs of raw Cambay amber, which has yielded approximately 550 arthropod inclusions, including diverse myrmecine, dolichoderine, and formicine ants. The raw piece was trimmed using a 4" diameter diamond-edged, water-fed trim saw, into a prism approximately 20 mm x 10 mm x 8 mm. It was then embedded in EpoTek 301B synthetic resin, to protect the amber and inclusion for final trimming. The piece was then trimmed much smaller, to maximize full dorsal and lateral views of the beetle and to minimize the amount of amber matrix between the beetle and amber surface. Finally, it was carefully ground and polished using a series of wet emory papers of decreasing grit sizes (400, 600, 800, 1200, 2400).

Confocal microscopy

For confocal imaging, a specimen of *Diartiger fossulatus* was incubated in DNA extraction buffer to dissolve soft tissues (recipe in [S48]), washed in ethanol and then disarticulated. Temporary slide preparations of body parts were made using Vectashield (Vector Labs) mounting medium. A Leica SP5 confocal microscope with a 488 nm laser was used to obtain image stacks of structures with a 1 mm step size between sections (typically 100-250 sections were needed, depending on the structure). Image stacks were collapsed in LAS AF to make maximum projections.

Montage photography

For habitus images of Pselaphinae (including Clavigeritae), specimens were incubated in DNA extraction buffer to relax and clean them. Appendages were spread and beetles were mounted on temporary points for photography with a Visionary Digital photomicrographic apparatus with Infinity optics and a Canon 60D camera. Photograph stacks were combined to produce montage images using Helicon Focus.

Filming of living Clavigeritae interacting with host ants

To our knowledge, interactions between Clavigeritae and their host ants have not been filmed before. We collected live *Fustiger* sp. from a natural population near Austin, Texas, together with workers of its *Nylanderia* sp. host ant. A beetle and some workers were placed into a plastic bottle cap with damp tissue paper flooring, and filmed using a USB digital microscope. Over the course of two days, we were able to capture several typical behaviours.

Morphological placement of *Protoclaviger*

To resolve *Protoclaviger*'s relationship to Clavigeritae, we scored 33 morphological characters from *Protoclaviger* and members of the three tribes of Recent Clavigeritae—Clavigerini, Colilodionini and Tiracerini. We also scored putative sister taxa from the tribes Pselaphini and Arhytodini [S17], and the "tyrine group" of tribes from Pselaphitae (equivalent to all Pselaphitae except Arhytodini and Pselaphini, which unpublished molecular work has revealed form a strongly supported monophyletic group; J. Parker, in preparation). In addition, we included further outgroup Pselaphinae belonging to the four other supertribes: Faronitae, Euplectitae, Goniaceritae and Batrisitae. Although monophyly of Euplectitae and Goniaceritae is doubtful [S9], our sole aim was to assess the phylogenetic position of *Protoclaviger*, and for this purpose these supertribes represent units of sufficient character state consistency. A character matrix was developed in Mesquite [S49] using outgroup character states corresponding to those seen in Protopselaphinae and allied taxa of the pselaphine lineage of omaliine group staphylinid subfamilies, following Newton and Thayer [S9] and further discussion by Chandler [S1]. Parsimony analyses were conducted using TNT [S50] (mult = tbr replic 10000 hold 1000 ratchet drift;) with all

characters treated as unordered multistate. Clade support was estimated by bootstrap [S51] (resample boot replic 10000;).

Character states indicated for a given higher taxon are those we could confidently conclude are ancestral within that taxon; when there was any doubt, we coded taxa with multiple states. Because of our focus on the placement of *Protoclaviger*, certain isolated examples of independently derived, homoplasious character state changes within higher taxa were disregarded, but we note these instances in the character descriptions below. Characters used by Newton and Thayer [S9] in their supertribal phylogeny of Pselaphinae are denoted "NT" followed by the character number as listed in that paper. Those used by Claude Besuchet [S17] or Ivan Lobl [S18] in their discussions of Clavigeritae relationships are denoted CB and IL, respectively.

1. Hind body width. Narrow, body approximately parallel sided (0). Broad, with both elytra and abdomen distinctly wider than head and prothorax (1).

2. Hind body convexity. Body form linear in profile, with pterothorax, elytra and abdomen relatively flattened, shallow in dorsoventral axis (0). Body form convex, with pterothorax, elytra and abdomen cylindrical or globular, long in dorsoventral axis with compact abdomen (1).

3. Fovea. Foveae (striated pit-like invaginations) absent on body (0). Fovea present on at least some body regions (1).

4. Squamous pubescence. Flattened, squamous-type pubescence entirely absent on body (0). Squamous pubescence present on some body regions (1).

5. Frontal rostrum. Absent or only weakly evident, with front of head broad between widely separated antennal bases that are not mounted on a raised projection between eyes (0). Pronounced, with narrowing of head to clypeus and antennal bases closely approximate, mounted on raised projection between eyes (1).

6. Antennal bases. Antennal bases largely exposed, visible in dorsal view (0). Antennae inserted under shelf-like projections (1). (NT_17)

7. Antennal scape length. Scape prominent, apical portion visible in dorsal view (0). Scape short, concealed in dorsal view (1). (CB_2/IL_2)

8. Antennomere number. Antenna with more than six antennomeres (0). Antenna with at most six antennomeres (1). (CB_2/IL_2)

9. Antennal apex. Apex of terminal antennomere rounded or acuminate (0). Antenna apically truncate (1). (CB_2/IL_2)

10. Antennal apical excavation. Apex of terminal antennomere lacking cavity (0). Antenna apically with setose apical cavity (1). (CB_2/IL_2). The apical cavity is missing in a few genera of Clavigeritae.

11. Mandibles recessed in buccal cavity. Not recessed, exposed to at least half mandible length (0). Recessed, at most only apical teeth visible externally beyond buccal cavity (1). (CB_3/IL_3)

12. Mandibular prostheca. Prostheca absent (0). Prostheca present (1). (NT_34)

13. Maxillary palpus apical (fifth) pseudosegment. Apical pseudosegment absent on palpomere IV (0). Digitiform pseudosegment present on palpomere IV (1). (NT_37). We follow Newton and Thayer (1995) in treating the unsclerotized, seta-like structure at the apex of the single-segmented clavigerite maxillary palpus as homologous to the apical 5th pseudosegment of other Pselaphinae.

14. Maxillary palpus size. Small to large, but extending outside buccal cavity (1). Scarcely visible, largely recessed inside buccal cavity (2). (CB_4/IL_4)

15. Maxillary palpus segment number (apparent). Maxillary palpus 4-segmented (not counting apical pseudosegment) (0). Palpi apparently 1-segmented (1). (CB_4/IL_4). Palpomere reduction in some myrmecophilous groups such as Ctenistini and Attapseniini of the tyrine lineage is evidently independently derived and ignored for the purposes of this analysis.

16. Pronotal antebasal sulcus or impression. Pronotum with transverse impression or well developed antebasal sulcus present (0). Prontoum without trace of transverse impression (1). (NT_53). See discussion in Chandler (2001) p 30 for a discussion of the polarity of this character.

17. Elytral sutural striae. Elytron lacking stria along suture (0). Sutural stria present (1). (NT_70)

18. Protrochanter length. Protrochanter length short, dorsal face of proximal femur nearly touching proccoxa (0). Protrochanter much longer, profemur and procoxa widely separated (1).

19. Mesotrochanter length. Mesotrochanter length short, dorsal face of proximal femur nearly touching mesocoxa (0). Mesotrochanter much longer, mesofemur and mesocoxa widely separated (1). (NT_84/CB_6/IL_6)

20. Metacoxal projection. Metacoxa projecting at articulation with metatrochanter (0). Metacoxae not projecting (1).

21. Metatrochanter length. Metatrochanter length short, dorsal face of proximal femur nearly touching metacoxa (0). Metatrochanter much longer, metafemur and metacoxa widely separated (1).

22. Metacoxal separation. Metacoxae contiguous (0). Metacoxae separated (1).

23. Tarsomere 2 length. Second tarsomere clearly longer than tarsomere 1 (0). Tarsomeres 1 and 2 subequal in length (1). Tarsomere 2 approaches the length of 1 in *Caccoplectus* (Arhytodini). (NT_83/CB_7/IL_7)

24. Tarsal claw number. Two equally-sized tarsal claws (0). Two unequally-sized tarsal claws (1). A single tarsal claw present (2). (NT_81)

25. Composite abdominal tergal plate. Plate absent, segment boundaries of abdominal tergites IV-VI (visible segments 1-3) distinct (0). Plate present, tergites IV-VI fused, their boundaries not apparent (1). (CB_8/IL_8). Fusion of tergites has occurred independently in the SE Asian *Plagiophorus* (Cyathigerini) and partial fusion is seen in some Neotropical genera of Gonicarini, and these are ignored in this analysis.

26. Basal abdominal excavation. Abdominal tergite IV (visible tergite 1) without deep excavation at base (0). Tergite IV basally excavate, with deep impression (1). (CB_8/IL_8). The basal excavation of Clavigeritae is independently approached in some Tyrini (e.g. *Ceophyllus*) and Attapseniini of the tyrine lineage.

27. Basal abdominal trichomes. Trichomes absent from base of abdomen (0). (CB_11/IL_11). Trichomes present (1). Trichomes are present in this body region sporadically outside Clavigeritae, in Attapseniini, Ctenistini, Trichonychini and Batrisini.

28. Abdominal lateral margins. Interfaces between segments IV-IV angulate in dorsal view, making the lateral abdominal margins appear discontinuous (0). Interfaces between segments IV-IV not angulate, near-seamless continuity between edges of paratergites producing lateral margins of abdomen that are smoothly rounded to almost straight (1).

29. Relative length of abdominal tergite IV. Segment IV subequal in length to segment V (0). Segment IV at least 1.3 times as long as than segment V (1). In Clavigeritae, the state can be assessed using the still-segmented paratergites flanking the composite tergal plate.

30. Sternite III and IV setal concentration. Basal abdominal impression (apex of sternite III/ base of sternite IV) without pronounced accumulation of setae (0). Basal impression of ventral abdomen setiferous (1). (NT_89)

31. Sternite VIII defensive gland. Medial, unpaired omaliine-type defensive gland present (0). Sternal gland absent (1). (NT_92)

32. Ventral abdominal intersegmental membranes. Intersegmental membranes long, equal to or greater than 1/10 sternite length (0). Intersegmental membranes short, less than $1/10^{th}$ sternite length (1).

33. Ventral abdominal intersegmental membrane pattern. Membrane with brick-wall pattern of minute sclerites (0). Brick-wall sclerite pattern absent (1). (NT_96)

The resulting morphological character matrix for TNT is shown in Table S1.

Molecular phylogenetic analysis and diversification of Clavigeritae

Taxon sampling. Taxa are listed in Table S2. We included representatives of the six supertribes of Pselaphinae, incorporating taxa that enabled us to use all Pselaphinae fossils at our disposal for molecular dating of nodes outside of Clavigeritae. Within Clavigeritae, we aimed for as much taxonomic coverage as possible to provide a reliable and unbiased estimate of Recent diversity from across the breadth of the supertribe. This was crucial for dating the supertribe's origin, and for making assessments about its pattern of diversification. Given that the majority of genera are extremely rare and known from one or a few specimens, we had to resort to pinned museum specimens for some critical groups. Ultimately, we were able to include 31 species (~10% of the total) representing 26 genera (~25% of the total), including the monobasic Tiracerini and 8/10 subtribes of by far the largest tribe, Clavigerini (only the likely-derived subtribes Lunillina and Disarthricerina were not included). Within Clavigerini we added increased sampling from the two larger subtribes Clavigerodina and Clavigerina, and the diverse Madagascan fauna. We could not obtain specimens of the rare, monobasic tribe Colilodionini, but as we explain in "Phylogenetics and Diversification of Clavigeritae", absence of this tribe does not, we think, significantly affect our conclusions. Hence, little of any consequence from the pre-existing taxonomy of Clavigeritae was left out of our analysis. Our data set thus included appropriate unbiased taxonomic, morphological and biogeographic coverage to enable us to gauge the group's temporal pattern of diversification. We were also able to provide some insights into relationships between genera, and test the validity of several Clavigerini subtribes.

DNA extraction and sequencing. Ethanol-preserved specimens were vacuum dried, and pinned specimens were removed from card points. Specimens were incubated whole, without destruction in an SDS/Proteinase-K-based extraction buffer (see [S48] for recipe) for 2 days at 55°C. Following digestion, specimens were removed, and supernatant was phenol-chloroform extracted following the protocol detailed in [S21]. Purified DNA was resuspended in Tris-EDTA. Clontech Advantage 2 polymerase was used to amplify gene fragments and an annealing temperature of 51°C was typically used in all PCR reactions, with only the extension time being varied depending on target amplicon length. Bands were excised from gels and ligated into TOPO-XL-PCR vector (Life Technologies), and transformed into DH5a cells. Colonies were miniprepped and test digested with EcoRI. Plasmids containing correct inserts were batch-sequenced with T7 and M13R primers using Macrogen Corp. (NY, USA). The following primer combinations were used (asterisks indicate primers designed for this study):

28s rRNA (~650-800 bp): (**28sDD** 5'-GGGACCCGTCTTGAAACAC / **28sFF** 5'-CACACTCC TTAGCGGAT)

18s rRNA (~1900-2140 bp): **(18s5'short*** 5'-CAACCTGGTTGATCCTGCC **/ 18s3'l** 5'-CACCTACGG AAACCTTGTTACGAC or for problematic taxa, the 3' end of the locus was targeted using **18sa2.0** 5'-ATGGTTGCAAAGCTGAAAC**)**

16s rRNA (~425-535 bp): **(16saR** 5'-CGCCTGTTTATCAAAAACAT / **16sb** 5'-CTCCGGT TTGAA CTCAGATCA or **16sb_3*** 5'-TTAATCCAACATCGAGGTCG)

cytochrome oxidase I (820 bp)*:* (**TL2-N-3014PAT** 5'-TCCAATGCACTAA TCTGCCATATTA / **C1-J-2183JERRY** 5'-CAACATTTATTTTGATTTTTTGG or **Jerry2nd*** 5'-GATTTTTTG GWCAYCCWGAAG)

wingless (~450-510 bp): (**wg550f** 5'-ATGCGTCAGGARTGYAARTGYCAYGGYA TGTC / **wgABRZ** 5'-CACTTNACYTCRCARCACCARTG with secondary PCR if necessary **wg578f** 5'-TGACNGTGAARACYTGCTGGATG / **wgABR** 5'-ACYTCGCAGCACCARTGGAA)

In our final matrix, >90% of taxa were sequenced for all five loci (Table S2).

Phylogenetic analysis. Sequences were aligned in MUSCLE [S52] with default parameters, and visually inspected in Se-Al with minimal editing. Model selection in jModeltest2 [S53] yielded the GTR+I+G model for the Wg, COI and 18s rRNA partitions, GTR+G for 16s rRNA, and SYM+G for 28s rRNA. Sequences were concatenated using Sequence Matrix, producing a 51-taxon matrix comprised of 5944 characters. Bayesian inference, partitioned by locus, was performed using MrBayes 3.2.2 [S54], available through the Cipres Science Gateway [S55]. Two MCMC runs of one cold and three hot chains (temperature parameter 0.2) were run until the standard deviation of split frequencies dropped below 0.01, which was reached after 5.1 million generations. Tracer [S56] was used to judge adequate sampling from the posterior distribution. The first 25% of trees were discarded as burn-in. The resulting consensus tree was rooted with Faronitae, the basal-most lineage of Pselaphinae based on morphological [S9] and molecular phylogenetic analyses [S21]. Faronitae's basal position is also unequivocally supported by a forthcoming multilocus phylogeny of the entire subfamily Pselaphinae (Parker, in prep).

Molecular dating. The rooted and fully resolved maximum clade credibility tree from the MrBayes analysis was created by combining log files in TreeAnnotator [S57]. Branch lengths were transformed to create an ultrametric tree conforming to dating priors in TreeEdit [S58]. The constraint tree was imported into BEAST [S57] for fossil calibration using separate Bayesian lognormal relaxed clocks [S59] for the mitochondrial and nuclear gene partitions. For our focal analysis (Analysis #1), we employed seven fossils and one ancient biogeographic event. For the fossil calibrations, fossil ages were used as offsets that defined hard minimum bounds on lognormal distributions. Because we could not justify *a priori* how stringent the soft maximum bounds of our lognormal distributions should be [S27], we employed relatively weak soft maxima to shape their tails (using a high standard deviation) but performed an additional analysis (Analysis #2) with tighter soft maxima to determine how this affected the results.

Analysis #1 used the dating priors listed below, with their hard minimum ages, the type of distribution followed by the mean (in real space) and standard deviation (if lognormal) in parentheses:

A) Arhytodini (52 Ma [S60], lognormal, 10.0, 1.0). An undescribed Arhtyodine in Cambay amber (AMNH TAD-23; Fig S3A). Although the two genera of Arhytodini included in our analysis (*Rhytus* and *Caccoplectus*) are closely allied and emerge as a monophyletic sister group to Pselaphini (Fig 4A, S2), the monophyly of Arhytodini as a whole is questionable [S1], and the tribe may paraphyletic with respect to Pselaphini. The phylogenetic position of some genera of

Arhytodini, including the undescribed Cambay fossil, is presently unresolved, raising the possibility that it could have diverged earlier with respect to the four genera that comprise the (Arhytodini, Pselaphini) clade in our tree. Accordingly, rather than placing fossil A at the ancestral node joining (Arhytodini, Pselaphini), we opted for a conservative placement at the ancestral node of ((Arhytodini, Pselaphini) Clavigeritae) (fossil placement configurations are shown in Fig S4H; see also the alternative placement of Fossil A in Figure S2). In Analysis #1, Fossil A is therefore redundant with *Protoclaviger* (Fossil E). However, we also performed an additional analysis (Analysis #5), in which Fossil A was placed at the less conservative position of the node joining (Arhytodini, Pselaphini) (Fig S4H).

B) Bythinini (99 Ma [S61], lognormal, 10.0, 1.0). Undescribed Bythinini in Burmese amber (AMNH Bu-248 and AMNH B-023; Fig S3B).

C) Bythinoplectini: Bythinoplectina (52 Ma [S60], lognormal, 10.0, 1.0). Undescribed Bythinoplectina in Cambay amber (AMNH TAD-130; Fig S3C).

D) *Caccoplectus* (20 Ma, lognormal, 5, 0.5). *Caccoplectus* in Dominican amber [S44]; also AMNH DR8-429, Fig S3D).

E) Clavigeritae (52 Ma [S60], lognormal, 10.0, 1.0). *Protoclaviger* in Cambay amber (AMNH TAD 490; Fig S3E).

F) Ctenistini (52 Ma [S60], lognormal, 10.0, 1.0). Undescribed Ctenistini in Cambay amber (AMNH TAD-491; Fig S3F).

G) *Faronus* (44 Ma, lognormal, 10.0, 1.0). *Faronus* in Baltic amber [S29] (and AMNH Ba-JWJ 334; Fig S3G).

H) “Higher Pselaphinae” (150 Ma, exponential, 20.0). The higher Pselaphinae are comprised of all Pselaphinae except the basal-most supertribe, Faronitae. The presence of non-faronite pselaphines in mid-Cretaceous Laurasian Burmese amber, combined with the evidently Gondwanan origin of many higher pselaphine tribes (inferred from their modern zoogeographic distributions), indicates the higher Pselaphinae likely originated on Pangaea, hence at the latest by the end of the Jurassic. We used a conservative date of 150 Ma and an exponential distribution with mean = 20.0 to incorporate uncertainty about when, before this minimum age, the higher Pselaphinae arose. Because we applied this date so close to the root, we did not specify a root height in our analysis.

Four independent BEAST runs of 200 million generations were performed using a speciation birth-death process tree prior [S62]. We enforced the tree topology during the analysis [S63], but also ran an identical analysis where topology was not enforced (Analysis #7). Convergence of runs was judged based on high ESS values in Tracer [S56]. Tree files were combined in LogCombiner with the first 10% of trees discarded as burn-in, yielding the time-calibrated maximum clade credibility tree shown in Figure 4A. The tree was imported into R (http://www.R-project.org) to produce the Lineages-Through-Time plot in Figure 4B using the Ape package [S64]. Data for the relative abundance of ants in different fossil deposits, used in Figure 4B, are from [S33] and [S65].

Six additional BEAST analyses were performed to explore how our priors influenced our results. These differ from Analysis #1 as follows:

Analysis #2. Tighter maximum bounds on fossil calibration densities. Standard deviations on all fossil calibrations (A-G) were lowered to 0.4 to constrain the variance of the soft maximum bounds of our dating priors.

Analysis #3. Molecular data excluded. Using overly-strict dating priors can override information from the molecular data, and strongly constrain estimation of the posterior [S27, 28]. An analysis run without any molecular data will sample from the prior alone, enabling one to gauge whether the priors used are dictating the outcome.

Analysis #4. All fossil calibrations excluded. To ascertain how are our fossil dating priors were influencing the outcome of our analysis, all our fossil calibrations (A-G) were removed, and only calibration H (higher Pselaphinae) was included.

Analysis #5. Alternative placement of fossil A. The impact of placing Fossil A at the less conservative, more recent ancestral node of (Arhytodini, Pselaphini) (scheme depicted in Fig S4H) was explored.

Analysis #6. Fossils A+E excluded. To assess how removal of *Protoclaviger* (Fossil E) and redundant Fossil A altered our inferences concerning dating of Clavigeritae, both E and A calibration points were excluded from the analysis (Fig S4H).

Analysis #7. Tree topology unconstrained. We determined the extent to which using a rigid constraint tree affected our analysis by running an otherwise identical analysis in which the topology was simultaneously estimated in BEAST.

Supplemental References

S1. Chandler, D. S. (2001). Biology, Morphology and Systematics of the Ant-Like Litter Beetles of Australia (Associated Publishers).

S2. Hlavac, P. (2011). Contribution to the knowledge of the tribe Mastigerina (Coleoptera: Staphylinidae: Pselaphinae, Clavigeritae), with a description of a new genus from Borneo. Zootaxa *3070*, 51–59.

S3. Krüger, E. (1910). Beiträge zur anatomie und biologie des *Claviger testaceus* Preyssl. Zeitschrift für wissenschaftliche Zoologie *95*, 327–381.

4. Hill, W., Akre, R., and Huber, J. (1976). Structure of some epidermal glands in the myrmecophilous beetle *Adranes taylori* (Coleoptera: Pselaphidae). Journal of The Kansas Entomological Society *49*, 367–384.

S5. Cammaerts, R. (1974). Le systeme glandulaire tegumentaire du coleoptere myrmecophile *Claviger testaceus* Preyssler, 1790 (Pselaphidae). Z. Morph. Tiere *77*, 187–219.

S6. Cammaerts, R. (1992). Stimuli inducing the regurgitation of the workers of *Lasius flavus* (Formicidae) upon the myrmecophilous beetle *Claviger testaceus* (Pselaphidae). Behav Process *28*, 81–96.

S7. Leschen, R. A. B. (1991). Behavioral observations on the myrmecophile *Fustiger knausii* (Coleoptera: Pselaphidae: Clavigerinae) with a discussion of grasping notches in myrmecophiles. Entomological News *102*, 215–222.

S8. Park, O. (1942). A Study in Neotropical Pselaphidae (Evanston and Chicago: Northwestern University).

S9. Newton, A. F., and Thayer, M. K. (1995). Protopselaphinae new subfamily for *Protopselaphus* new genus from Malaysia, with a phylogenetic analysis and review of the Omaliine Group of Staphylinidae including Pselaphidae (Coleoptera). In *Biology, Phylogeny, and Classification of Coleoptera: Papers Celebrating the 80th Birthday of Roy A. Crowson.*, J. Pakaluk and S. A. Slipinski, eds. (Muzeum i Instytut Zoologii PAN, Warszawa), pp. 221–320.

S10. Jeannel, R. (1936). Monographie des Catopidae (Insectes Coléopteres). Mémoires du Muséum National d'Histoire Naturelle N.S. *1*, 1–438.

S11. Geiselhardt, S. F., Peschke, K., and Nagel, P. (2007). A review of myrmecophily in ant nest beetles (Coleoptera: Carabidae: Paussinae): linking early observations with recent findings. Naturwissenschaften *94*, 871–894.

S12. Jałoszyński, P. (2013). A new species of the putatively myrmecophilous genus *Plaumanniola* Costa Lima, with notes on the systematic position of Plaumanniolini (Coleoptera: Staphylinidae: Scydmaeninae). Zootaxa *3670*, 317.

S13. Schomann, A., Afflerbach, K., and Betz, O. (2008). Predatory behaviour of some Central European pselaphine beetles (Coleoptera: Staphylinidae: Pselaphinae) with descriptions of relevant morphological features of their heads. European Journal of Entomology *105*, 889–907.

S14. Ohishi, H. (2000). Notes on the mouthparts of Pselaphinae (Coleoptera: Staphylinidae). Insecta Miyatakeana, a special publication from the Entomological Laboratory, Osaka Museum of Natural History, 37–46.

S15. Lobl, I. (2000). *Pachacuti chandleri* sp. n. and *Sabarhytus kinabalu* gen. et sp. n. with comments on Arhytodini and Pselaphini (Coleoptera, Staphylinidae, Pselaphinae). Biological Journal of the Linnean Society *55*, 143–149.

S16. Park, O. (1932). The myrmecocoles of *Lasius umbratus mixtus aphidicola*

Walsh. Ann Entomol Soc Am *25*, 77–88.

S17. Besuchet, C. (1991). Révolution chez les Clavigerinae (Coleoptera, Pselaphidae). Rev. Suisse Zool. *98*, 499–515.

S18. Lobl, I. (1994). The Systematic Position of Colilodionini with Description of a New Species (Coleoptera, Pselaphidae). Revue Suisse de Zoologie *101*, 289–297.

S19. Nomura, S., and Sugaya, H. (2007). A New Species of the Genus *Colilodion* Besuchet (Coleoptera: Staphylinidae: Pselaphinae) from Vietnam. Annales de la Société Entomologique de France (n.s.) *43*, 333–339.

S20. Zhao, M.-J., Yin, Z.-W., and Li, L.-Z. (2010). Contributions to the knowledge of the myrmecophilous pselaphines (Coleoptera, Staphylinidae, Pselaphinae) from China. IV. The second species of the genus *Songius* (Coleoptera, Staphylinidae, Pselaphinae), with description of its probable mature larva. Sociobiology *56*, 77–89.

S21. Parker, J., and Maruyama, M. (2013). *Jubogaster towai*, a new Neotropical genus and species of Trogastrini (Coleoptera: Staphylinidae: Pselaphinae) exhibiting myrmecophily and extreme body enlargement. Zootaxa *3630*, 369–378.

S22. Zi-Wei Yin, L.-Z. L. (2013). *Pengzhongiella daicongchaoi* gen. et sp. n., a remarkable myrmecophile (Staphylinidae, Pselaphinae, Batrisitae) from the Gaoligong Mountains. Zookeys *326*, 17–26.

S23. Jeannel, R. (1954). Les Pselaphides de Madagascar. Memoires de l'Institut Scientifique de Madagascar *4*, 139–344.

S24. Celis, M. J. (1969). Contribution á l'etude des Clavigerinae de l'Afrique (Coleoptera Pselaphidae) 3. Démembremant des Fustigerini et création de deux tribus nouvelles ainsi que d'un genre inédit. Revue de Zoologie et de Botanique Africaines *80*, 415–424.

S25. Besuchet, C. (2008). Synonymies et combinaisons nouvelles, revalidations et description de taxa nouveaux de Pselaphinae (Coleoptera: Staphylinidae). Mitteilungen der Schweizerischen Entomologischen Gesellschaft *81*, 61–82.

S26. Hlaváč, P., Baňař, P., and Parker, J. (2013) The Pselaphinae of Madagascar. II. Redescription of the genus *Semiclaviger* Wasmann, 1893 (Coleoptera: Staphylinidae: Pselaphinae: Clavigeritae) and synonymy of the subtribe Radamina Jeannel, 1954. Zootaxa *3736*, 265.

S27. Ho, S. Y. W., and Phillips, M. J. (2009). Accounting for Calibration Uncertainty in Phylogenetic Estimation of Evolutionary Divergence Times. Syst. Biol. *58*, 367–380.

S28. Heled, J., and Drummond, A. J. (2012). Calibrated tree priors for relaxed phylogenetics and divergence time estimation. Syst. Biol. *61*, 138–149.

S29. Schaufuss, L. W. (1890). System-schema der Pselaphiden, ein Blick in die Vorzeit, in die Gegenwart und In die Zukunft. Tijdschrift voor Entomologie *33*, 101–162.

S30. Wasmann, E. (1929). Die Paussiden des baltischen Bernsteins und die Stammesgeschichte der Paussiden. In Bernstein-Forschungen (Amber studies), K. Andrée, ed., pp. 1–110.

S31. Wappler, T. (2003). Systematik, Phylogenie, Taphonomie und Paläoökologie der Insekten aus dem Mittel-Eozän des Eckfelder Maares, Vulkaneifel. Clausthaler Geowissenschaften *2*, 1–241.

S32. Wheeler, W. M. (1914). The ants of the Baltic amber. Schriften der Physikalisch-okonotnischen Gesellschaft Königsberg *55*, 1-142.

S33. Grimaldi, D., and Agosti, D. (2000). A formicine in New Jersey Cretaceous

amber (Hymenoptera : Formicidae) and early evolution of the ants. Proc. Natl. Acad. Sci. U.S.A. *97*, 13678–13683.

S34. Wilson, E. O., and Hölldobler, B. (2005). The rise of the ants: A phylogenetic and ecological explanation. Proceedings of the National Academy of Sciences *102*, 7411–7414.

S35. Heraty, J. M., and Darling, D. C. (2009). Fossil Eucharitidae and Perilampidae (Hymenoptera: Chalcidoidea) from Baltic Amber. Zootaxa *2306*, 1–16.

S36. Sohn, J. C., Labandeira, C., Davis, D. R., and Mitter, C. (2012). An annotated catalog of fossil and subfossil Lepidoptera (Insecta: Holometabola) of the world. Zootaxa *3286*, 1–132.

S37. Hull, F. M. (1945). A revisional study of the fossil Syrphidae. Bulletin of The Museum of Comparative Zoology *95*, 251–355.

S38. Nagel, P. (1997). New fossil paussids from Dominican amber with notes on the phylogenetic systematics of the paussine complex (Coleoptera: Carabidae). System Entomol *22*, 345–362.

S39. Kraemer, M. M. S. (2006). The first fossil paussine (Coleoptera: Carabidae) from Mexican amber. Paläontol Z *80*, 107–111.

S40. Tishechkin, A. K. (2005). Phylogenetic Revision of the Genus *Mesynodites* Reichardt (Coleoptera: Histeridae: Hetaeriinae). Dissertation. (Louisiana State University).

S41. Engel, M. S., and Chatzimanolis, S. (2009). An oxyteline rove beetle in dominican amber with possible African affinities (Coleoptera: Staphylinidae: Oxytelinae). Annals of Carnegie Museum *77*, 425–429.

S42. Martins-Neto, R. G. (1991). Sistemática dos Ensifera (Insecta, Orthopteroida) da formação Santana, Cretáceo Inferior do Nordeste do Brasil. Acta Geologica Leopoldensia *32*, 5–160.

S43. Chandler, D. S. (1975). A Revision of the Genus *Caccoplectus* (Coleoptera: Pselaphidae). The Coleopterists Bulletin *29*, 301–316.

S44. Chandler, D. S., and Wolda, H. (1986). Seasonality and diversity of *Caccoplectus*, with a review of the genus and description of a new genus, *Caccoplectinus* (Coleoptera: Pselaphidae). Zoologische Jahrbiicher. Abteilung flir Systematik, Okologie und Geographie *113*, 469–524.

S45. Bruch, C. (1918). Nuevos huéspedes de hormigas procedentes de Córdoba. Physis *4*, 186–195.

S46. Peris, D., Chatzimanolis, S., and Delclòs, X. (2014). Diversity of rove beetles (Coleoptera: Staphylinidae) in Early Cretaceous Spanish amber. Cretaceous Research *48*, 85–95.

S47. Newton, A. F., and Chandler, D. S. (1989). World catalog of the genera of Pselaphidae (Coleoptera). Fieldiana Zoology *53*, 1–110.

S48. Gilbert, M. T. P., Moore, W., Melchior, L., and Worobey, M. (2007). DNA Extraction from Dry Museum Beetles without Conferring External Morphological Damage. PLoS ONE *2*, e272.

S49. Maddison, W. P., and Maddison, D. R. (2011). Mesquite: a modular system for evolutionary analysis. Version 2.75. mesquiteproject.org.

S50. Goloboff, P. A., Farris, J. S., and Nixon, K. C. (2008). TNT, a free program for phylogenetic analysis - Goloboff - 2008 - Cladistics - Wiley Online Library. Cladistics *24*, 774–786.

S51. Felsenstein, J. (1985). Confidence-Limits on Phylogenies - an Approach Using the Bootstrap. Evolution *39*, 783–791.

52. Edgar, R. C. (2004). MUSCLE: multiple sequence alignment with high accuracy and high throughput. Nucleic Acids Res. *32*, 1792–1797.

53. Darriba, D., Taboada, G. L., Doallo, R., and Posada, D. (2012). jModelTest 2: more models, new heuristics and parallel computing. Nat. Methods *9*,

772.
54. Ronquist, F., Teslenko, M., van der Mark, P., Ayres, D. L., Darling, A., Höhna, S., Larget, B., Liu, L., Suchard, M. A., and Huelsenbeck, J. P. (2012). MrBayes 3.2: efficient Bayesian phylogenetic inference and model choice across a large model space. Syst. Biol. *61*, 539–542.
S55. Miller, M. A., Pfeiffer, W., and Schwartz, T. (2010). Creating the CIPRES Science Gateway for Inference of Large Phylogenetic Trees. In, M. A. Miller, W. Pfeiffer, and T. Schwartz, eds. (New Orleans), pp. 1–8.
S56. Rambaut, A., Suchard, M. A., Xie, D., and Drummond, A. J. (2013). Tracer v1.5. Available from http://beast.bio.ed.ac.uk/Tracer.
S57. Drummond, A. J., Suchard, M. A., Xie, D., and Rambaut, A. (2012). Bayesian Phylogenetics with BEAUti and the BEAST 1.7. Mol. Biol. Evol. *29*, 1969–1973.
S58. Rambaut, A., and Charleston, M. (2002). TreeEdit. Phylogenetic Tree Editor. tree.bio.ed.ac.uk.
S59. Drummond, A. J., Ho, S. Y. W., Phillips, M. J., and Rambaut, A. (2006). Relaxed phylogenetics and dating with confidence. PLoS Biol. *4*, e88.
S60. Rust, J., Singh, H., Rana, R. S., McCann, T., Singh, L., Anderson, K., Sarkar, N., Nascimbene, P. C., Stebner, F., Thomas, J. C., et al. (2010). Biogeographic and evolutionary implications of a diverse paleobiota in amber from the early Eocene of India. Proc. Natl. Acad. Sci. U.S.A. *107*, 18360–18365.
S61. Shi, G., Grimaldi, D. A., Harlow, G. E., Wang, J., Wang, J., Yang, M., Lei, W., Li, Q., and Li, X. (2012). Age constraint on Burmese amber based on U-Pb dating of zircons. Cretaceous Research *37*, 155–163.
S62. Gernhard, T. (2008). The conditioned reconstructed process. Journal of Theoretical Biology *253*, 769–778.
S63. Moreau, C. S., and Bell, C. D. (2013). Testing the museum versus cradle tropical biological diversity hypothesis: phylogeny, diversification, and ancestral biogeographic range evolution of the ants. Evolution *67*, 2240–2257.
S64. Paradis, E., Claude, J., and Strimmer, K. (2004). APE: Analyses of Phylogenetics and Evolution in R language. Bioinformatics *20*, 289–290.
S65. LaPolla, J. S., and Dlussky, G. M. (2013). Ants and the Fossil Record. Annu. Rev. Entomol. *58*, 609–630.
S66. Dunlop, J. A., Kontschán, J., Walter, D. E., and Perrichot, V. (2014). An ant-associated mesostigmatid mite in Baltic amber. Biol. Lett. *10*, 20140531